New Method for the Synthesis of Polyether-Bridged Azulenes: Reactions of Conjugated Ketocarbenes Generated from the Corresponding Azulenoquinone Diazides

Yun-Shan Lin,* Shuan-Ya Jiang, Tian-Chyuan Huang,[†] Shih-Jue Lin, and Yuan L. Chow*,[‡]

Department of Chemistry, Tamkang University, Tamsui, 25137, Taiwan

Received December 18, 1997

The diazide of 2,4-azulenoquinone carrying 1,3-cyano and carbomethoxy substituents was synthesized and photolyzed in cyclic ethers (THF, dioxane, and tetrahydropyran) to give good yields of 2,4-polyether-bridged azulenes. The shapes of some azulene polyethers were examined by X-ray structural determination to show the cavity size ranging from 6.4 to 4.1 Å (long−short diameters) to 7.36−6.6 Å encircled by an azulene and polyether arc. In analogy to 2,5-cyclohexadien-4-onylidenes, photogenerated conjugated azulenone carbenes were assumed to have energetically closely spaced triplet and singlet ground states that can interconvert readily and react from one of these states under ambient conditions. The spanning of a polyether bridge is initiated by the electrophilic attack of a singlet state on the oxygen of solvent ethers, followed by one or two propagation steps and a ring closure by phenolate attack. The 1,3-dicarbomethoxy group could exert steric effects to hinder the approach of the ether oxygen and control the polyether spanning processes and ring size; this caused a triplet state reaction to supersede the overall reaction. While radical and insertion reactions are common for ketocarbene reactions, the present description adduces a well manifested electrophilic reaction of the allied transients.

Introduction

The diazides of arenoquinones, such as benzoquinones, naphthoquinones, and anthraquinones, possess an unusual electronic structure in which the keto and diazo functions are doubly conjugated by vinylogues that endow a wide range of stability and reactivity.[1−3] These diazides are known to be the resonance hybrid of the contributing canonical structures of conjugated diazoketones and diazonium phenolates.[1] They are not only convenient precursors for reactive intermediates of conjugated ketocarbenes in synthetic applications[1,4] but also find commercial applications as photolithographic materials and polymer stabilizers.[1] Decomposition of these diazides by thermolysis or photolysis eliminates nitrogen to generate the corresponding conjugated ketocarbenes as transients[4] that can react interchangeably as radicaloid, carbenoid, and/or ionic types.[5−8] A number of such diazides has been photolyzed in argon matrices at 10 K to generate the matrix-isolated ketocarbenes that are characterized by IR, ESR, and UV spectroscopy.[4] They have been studied by laser flash photolysis to give transient absorption spectra and the decay kinetics.[5] These data have been interpreted such that the transient possesses the phenoxy radical structure and, by implications, the triplet ground state.[4,5] The chemical reactions of these species with alkane, alcohol, and olefin substrates showed typical radical or carbene-type reactions.[5−8]

Taking advantage of the ready availability of carbalkoxy- and cyano-substituted azulene derivatives, we,[6] as well as others,[7] have prepared diazoazulenoquinones (DAQ) **1** and **3a** and studied their photochemical reactions. Both DAQ **1a** and **1b** in solution undergo photoreactions that can be best interpreted as those arising from radical and carbene intermediates.[6a,7a] Significantly, the photoreaction of **1a** in and with tetrahydrofuran (THF) has led to an insertion of the ketocarbene entity into the O-C bond to give a 2,6-polyether bridged azulene,[8] such as **2b-4THF**. This reaction constitutes a new methodology potentially useful to span a polyether bridge across the azulene ring at the original quinoid termini. This paper reports successful applications of this photoreaction to DAQ **3** wherein good yields of polyether-bridged azulenes are synthesized. As these macrocyclic polyethers azulenes should show the tendency of accommodating various guests[9,10] in their cavity, they are potentially applicable to constructing chemical

---

[†] Present address: National Taipei College of Nursing, Taipei 11211, Taiwan.

[‡] Visiting Professor from Simon Fraser University, Burnaby, British Columbia, Canada.

(1) Ershov, V. V.; Nikiforov, G. A.; De Jonge, C. R. H. I. *Quinone Diazides*; Elsevier: Amsterdam, 1981.

(2) Sander, W.; Bucher, G.; Komnick, G.; Morawietz, J.; Bubenitschek, P.; Jones, P. G.; Chrapkowski, A. *Chem. Ber.* **1993**, *126*, 2101.

(3) Nozoe, T.; Asao, T.; Yasunami, S.; Wakui, H.; Suzuki, T.; Ando, M. *J. Org. Chem.* **1995**, *60*, 5919.

(4) (a) Sander, W.; Bucher, G. *J. Org. Chem.* **1992**, *57*, 1346. (b) Sander, W.; Bucher, G.; Reichel, F.; Cremer, D. *J. Am. Chem. Soc.* **1991**, *113*, 5311. (c) Sander, W.; Mueller, W.; Sustmann, R. *Angew. Chem., Int. Ed. Engl.* **1982**, *27*, 572.

(5) (a) Field, K. W.; Schuster, G. B. *J. Org. Chem.* **1988**, *53*, 4000. (b) Arnold, B. R.; Scaiano, J. C.; Bucher, G. F.; Sander, W. W. *J. Org. Chem.* **1992**, *57*, 6469.

(6) (a) Wun, W.-C.; Huang, T.-C.; Lin, S.-J.; Lin, B.-B.; Morita, T.; Lin, Y.-S. *J. Chin. Chem. Soc.* **1993**, *40*, 503. (b) Huang, T.-C.; Morita, T.; Lin, B.-B.; Lin, Y.-S. *J. Chin. Chem. Soc.* **1994**, *41*, 199. (c) Huang, T.-C.; Jiang, S.-Y.; Lin, Y.-S. *Taiwan Kexue* **1996**, *49*, 38.

(7) (a) Takase, K.; Morita, T. *Chem. Lett.* **1977**, 513. (b) Walch, S. P.; Goddar, W. A., III. *J. Am. Chem. Soc.* **1975**, *97*, 5319. (c) Takagi, K.; Mizuno, A.; Joyama, T.; Tsuji, T.; Wakabayashi, H.; Nozoe, T. *Chem. Exp.* **1992**, *7*, 25. (d) Nozoe, T.; Asao, T.; Susumago, M.; Ando, M. *Bull. Chem. Soc. Jpn.* **1974**, *47*, 1974.

(8) Nozoe, T.; Huang, T.-C.; Shyr, M.-H.; Lin, Y.-S.; Takeshita, H. *Synlett* **1995**, 952.

(9) Lehn, J.-M. *Angew. Chem., Int. Ed. Engl.* **1990**, *29*, 1304.

(10) Fabbrizzi, L.; Poggi, A. *Chem. Soc. Rev.* **1995**, 197.

(11) Czarnik, A. W., Ed. *Fluorescent Chemosensers for Ion and Molecule Recognition*; ACS Symposium Series 538; American Chemical Society: Washington DC, 1993.

S0022-3263(97)01494-1 CCC: $15.00

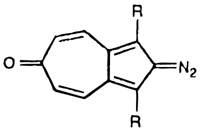

1 b : R = CN
C : R = CO_2CH_3

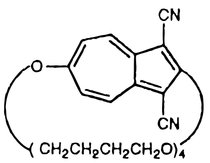

2b-4THF

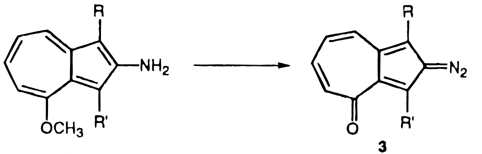

4

3

a : R = CO_2CH_3, R' = CN
b : R = R' = CN
C : R = R' = CO_2CH_3

devices for molecular recognition and information sensing.[9–11]

Results

The desired carbomethoxy- and cyano-substituted 2-diazo-2,4-azulenoquinones (DAQ; **3a**−**c**) were prepared according to the procedure used previously[6] to prepare the allied 2-diazo-2,6-azulenoquinones (**1**), by the nitrosation of the corresponding substituted 2-amino-4-methoxyazulenes (**4**). DAQ **3** were isolated as orange-red crystals and characterized by spectroscopic data and, in one case (that of **3a**), by single-crystal X-ray analysis.[6c] The samples of DAQ **3** exhibited the expected spectral properties as described in the Experimental Section. DAQ **3a** has been reported in detail recently;[3] the physical data of our preparations compare well with those reported.

Photolysis of DAQ **3a** was carried out in tetrahydrofuran under nitrogen irradiated with a 300 nm light source (RPR-3000 Å lamps) until the complete consumption of DAQ, which generally required about 4-6 h. The crude products were chromatographed on silica gel to give the compounds of an azulene skeleton incorporated with two and three THF molecules (**5a-2THF** and **5a-3THF**) as the major products in 16 and 71% yield, respectively, in addition to trace amounts of minor products that were not isolated (Scheme 1). DAQ **3b** was similarly photodecomposed in THF under nitrogen and worked up to afford **5b-2THF** and **5b-3THF** in 11 and 76% yields, respectively. The structures of these **5a** and **5b** were determined primarily from mass spectrometric molecular weight by the FAB mode to indicate the incorporation of THF and supported by the pertinent NMR, IR, and UV data given in the Experimental Section. These spectroscopic data unambiguously expressed the presence of cyano, carbomethoxy, azulenoid, and ether groups integrated in these molecules; their comparisons and rationalization will be expanded below. The structures of **5a-2THF** and **5a-3THF** were confirmed unequivocally by X-ray structural analysis of singl crystals (Figure 1); this also revealed their solid-state molecule shape.

DAQ **3a** and **3b** were photolyzed under comparable conditions in tetrahydropyran (THP) under nitrogen to given the major products **5a-2THP** and **5b-2THP**, respectively, in 75 and 72% yields. Similar photolysis of DAQ **3a** and **3b** in nitrogen-saturated dioxane (DXN) also gave single major products **5a-2DXN** and **5b-2DXN** in 79 and 76% yield, respectively, in each case. The products showed the pertinent spectral data, and the structures of **5b-2THP**, **5a-2DXN**, and **5b-3DXN** were also determined by X-ray analysis. The sole products obtained in these cases as well as mixtures in the above cases were those derived from spanning two or more linear units of ether (THF, THP, or DXN) molecules across the 2,4-position of the azulene nucleus; i.e., a multiple insertion of the 2,4-ketocarbene termini (see **10** below) in series into the ether C−O bond.

Scheme 1

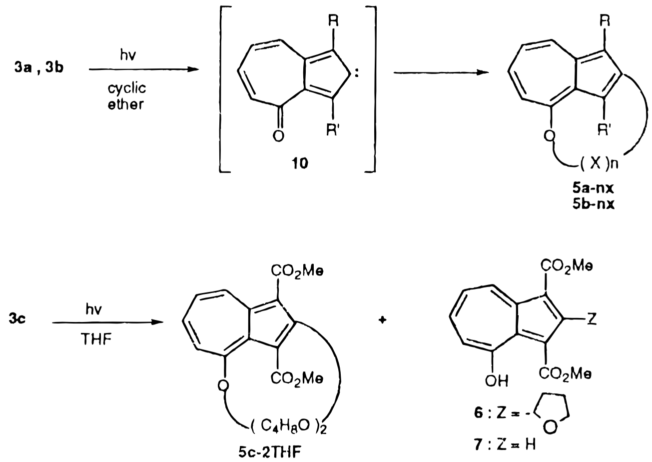

When **3c** was photolyzed in THF solution under nitrogen, it gave only 17% of **5c-2THF** but more azulenols **6** and **7** (19 and 36% yield). The formation of **7**, in theory, required a reduction step with two hydrogen atoms. While its formation had some precedent analogies in other diazo azulenoquinone photoreactions,[6a,7c] that as the major product was unexpected. The source of two hydrogen atoms was assumed to be THF that required the byproduct of dehydrotetrahydrofurans; their presence was, however, not confirmed. The structure was confirmed by the NMR singlet at 8.58 ppm for the H-2 and the molecular ion at 261 for $M^+ + 1$. Both **6** and **7** show comparable UV and NMR spectra, except that the H-8 doublet shows a large chemical shift difference at 8.08 and 9.62 ppm. This suggests that the former **6** has the C-1 carbomethoxyl group constrained to orient orthogonal to the azulenoid π-plane owing to the steric crowding of the C-2 tetrahydrofuran group; as the result, the H-8 is placed on the shielding cone of the ester group.

As these azulene polyethers are unsymmetrical coordinating macrocycles, the representative ones have been recrystallized to afford X-ray-quality crystals for structural determination; the details of the working parameters and their bonds and angles are summarized in tables as Supporting Information. Additionally, the ORTEP drawing of the structure of these macrocyclic polyethers, except those of **5a-2THF** and **5a-3THF** shown in Figure 1, are also available in the Supporting Information. Their molecular shape could be evaluated from the dihedral angles at the azulenol C−O bond at C-2 and C-4, and the longest and shortest distances of the elliptic cavity as summarized in Table 1. These data indicate that in the solid state these polyether macrocycles, except **5a-3THF**, possess the azulenoid π-plane slanted, but not perpendicular, to the polyether arc. As **5a-3THF** has a larger polyether arc (see Figure 1), it

---

(12) Lin, I.-W.; Huang, T.-C.; Lin, Y.-S. Unpublished results.

(13) (a) Harrison, J. F.; Liedtke, R. C.; Liebman, *J. Am. Chem. Soc.* **1979**, *101*, 7162. (b) Baird, N. C.; Taylor, K. F. *J. Am. Chem. Soc.* **1978**, *100*, 1333.

(14) Moss, R. A. *In Carbenes*; Jones, M., Jr., Moss, R. A., Eds.; John Wiley: New York, 1973; pp 153−304.

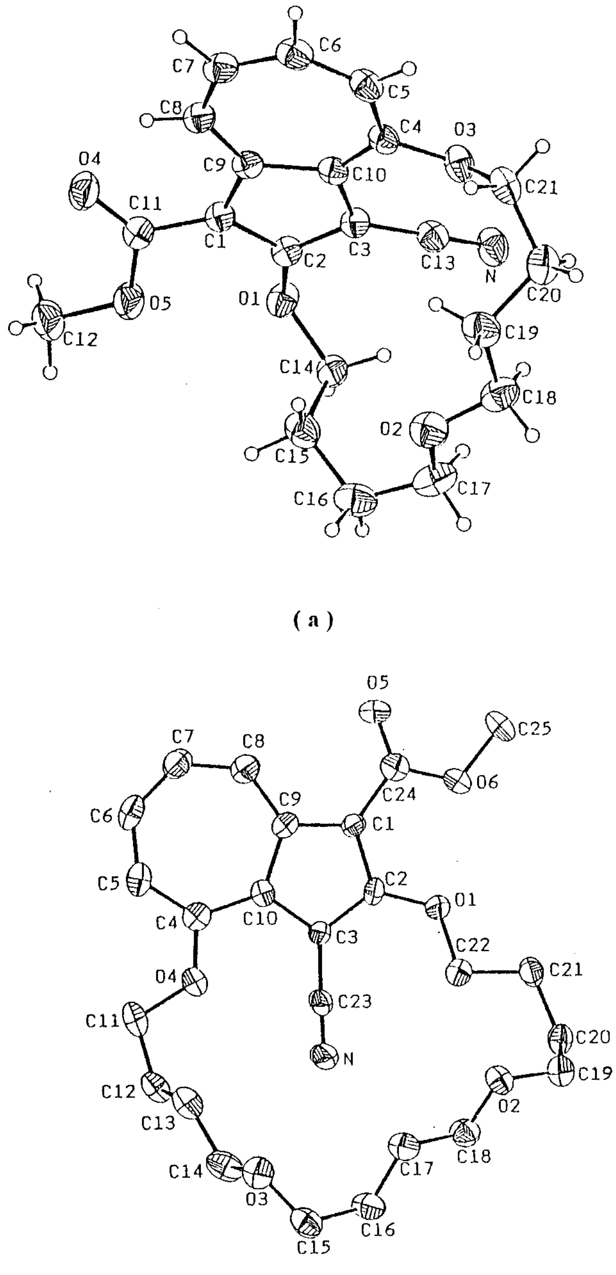

Figure 1. X-ray structure (ORTEP drawings) for (a) **5a-2THF** and (b) **5a-3THF**.

exhibits a nearly flat molecular shape wherein the π-plane is approximately coplanar with the cycle. This, in contrast to **5a-2THF**, is believed to be general and also applicable to the **5b** series. These solid-state structures could serve as reference to facilitate the interpretations of physical data.

The MS data of these products **5a**−**c** were readily interpretable in terms of the elimination of either a CH_3O group (*m*/*e* 31) or incorporated ether units (e.g., *m*/*e* 72 for THF, 86 for THP, 88 for DXN) in sequence. Both ^{13}C and ^{1}H NMR spectra clearly indicated the presence of the azulene ring and polyether bridge. It is particularly instructive to find the azulenoxy-CH_2 signals spread in 4.3−5.0 ppm and other alkylether-CH_2 signals in the 3.5 ppm region. The most significant contrast in ^{1}H NMR spectra is that observed between products **5a**−**c** incorporated with two THF and those with three THF; the former showed well-resolved multiplet signals for each proton of ether-CH_2 groups, and the latter exhibited sharp triplets for each ether-CH_2 groups. The difference in spectral patterns undoubtedly indicated rapid conformational mobility (on the NMR time scale) of the larger 3THF polyether span in **5a,b** but slow mobility or, more likely, a relatively hindered and immobile conformation for the smaller 2THF span in **5a**−**c**. In view of the solid-state structure of **5a-2THF** and **5a-3THF** (see Figure 1), the structure with two THF groups is assumed to have a locked conformation and that with three THF groups a freely flexible one in solution. In the solid state the latter must exist in the most stable and averaged-out conformation as shown in Figure 1.

Table 1. Torsional Angles at the Azulenoic C2−O and C4−O Bonds and Cavity Sizes[a]

compd	CH_2−O−C2−C1[b]	CH_2−O−C4−C5[b]	inner distances (Å)
5a-2THF	48.0	44.9	6.38−4.09
	(49.0)[c]	(46.4)[c]	
5a-3THF	10.5	0.8	7.31−6.59
5b-2THP	52.4	26.2	7.09−5.31
	(50.7)[c]	(28.5)[c]	
5a-2DXN	57.1	29.0	6.43−5.01
5b-2DXN	51.4	32.3	6.41−4.98

[a] The estimated cavity sizes are given for the longest and shortest distance in Å. [b] The C1−C5 stand for the carbon numbering of the azulene nucleus and CH_2O is that attached to the C2 and C4 position. [c] These data are those from the alternative structure in crystal cell.

Discussion

The photodecomposition of **1a** and the reaction of the corresponding conjugated ketocarbene with ether-type substrates is currently under investigation,[12] which includes reinvestigation on the detail of the reaction with THF to give 2,6-polyether-bridged azulene compounds.[8] In comparison, the results described above are cleaner and demonstrate that the photolysis of **3a,b** in cyclic ethers as solvent could lead to the formation of the corresponding 2,4-polyether-bridged azulenes in synthetically useful yields that should arise from the intermediacy of the corresponding conjugated 2,4-ketocarbenes, such as **10** or its valence isomers[6,8] in Scheme 2, in analogy to the previous observation from this group. The low yield of the allied polyether **5c-2THF** appears to be caused by steric crowding and should provide a key to elicit the actual reacting intermediate that will be elaborated below. From the overall reaction pattern, the process of spanning polyether bridges across a molecular π-plane shown above constitutes an insertion reaction of conjugated ketocarbenes (or their valence isomers **8**−**12**) into the C−O single bond of ethers as shown in Scheme 2, in which the key step is the excitation to cause the nitrogen elimination of the corresponding quinone diazides. As the matter of practical, mechanistic, and theoretical interests, the reaction could be discussed on the basis of Scheme 2.

On the basis of extensive studies on carbenes,[13,14] ketocarbenes[15] and conjugated ketocarbenes (such as 2,4-cyclohexadienon-4-ylidenes),[4,5,16] the ground state of the

---

(15) (a) Noyori, R.; Yamanaka, M. *Tetrahedron Lett.* **1980**, 2851. (b) Christensen, L. W.; Waali, E. E.; Jones, W. M. *J. Am. Chem. Soc.* **1972**, *94*, 2118.

(16) (a) Wasserman, E.; Murray, R. W. *J. Am. Chem. Soc.* **1964**, *86*, 4203. (b) Koser, G. F. *J. Org. Chem.* **1977**, *42*, 1474.

Scheme 2

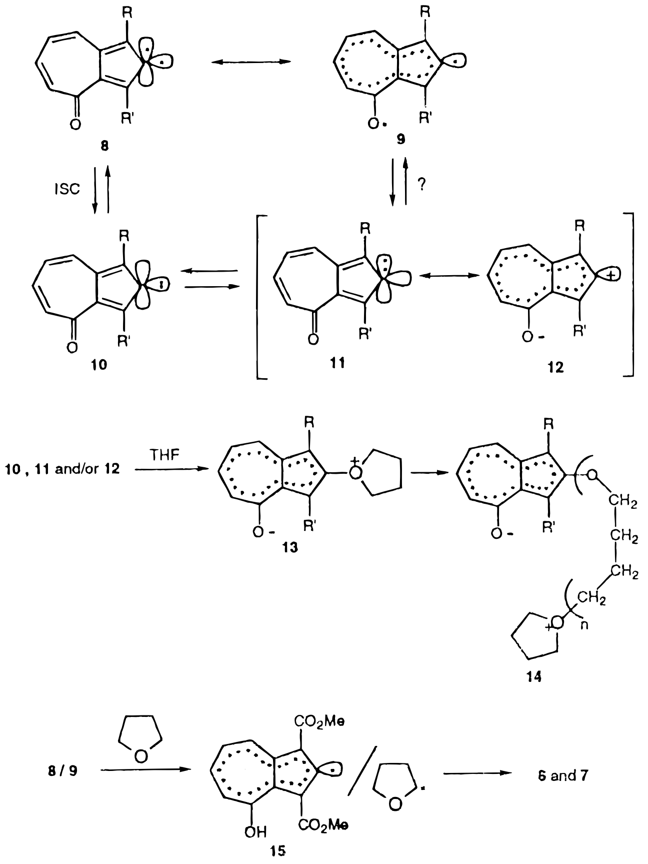

conjugated ketocarbenes derived from **3** must be in the triplet state, such as the resonance hybrid of **8** and **9** (see Scheme 2), which should possess the lowest energy level aided by the one-electron delocalization; the triplet state is assigned as the σp state since two electrons with parallel spin are accommodated one each in the σ- and p-orbitals respectively at C-2. The assignment is based on the conclusions reached from the study of ESR[16] and absorption spectra in low-temperature matrices[4] and in solution at ambient temperatures by flash photolysis.[5] While the results from semiempirical LCAO computations with the Huckel approximation are ambiguous, recent ab initio MO calculations on 2,5-cyclohexadienon-4-ylidene[17] provide an important link to our discussion below. The conventional singlet state **10** (the closed-shell singlet) has the pair of spin-coupled electrons localized in the σ-orbital at the C-2 position (i.e., σ^2-state), which inevitably lacks resonance stabilization; the energy level must be much higher than **8**/**9**. The transition from the triplet state **8**/**9** by the promotion and spin inversion of the σ-electron reaches another singlet state **10**/**11** with the spin-coupled electron pair in the p-orbital (i.e., the p^2-state). Intuitively, we assume that the energy gain of the delocalization (i.e., to attain the aromatic form of vinylcarbonium-phenolate species **12**) largely compensates the required transition energy. In view of the usually substantial aromatization energy gains, we propose that the **11**/**12** singlet state (p^2-state) possesses an energy level much lower than the other singlet **10** (σ^2-state) and close to the ground triplet state **8**/**9** (σp-state). It follows that conjugated ketocarbenes generated from **3** are most likely to react from either the triplet state **8**/**9** or the singlet state **11**/**12** interconvertibly and that the σ^2-state **10** is not likely to figure as an important reactive species under ambient conditions as in Scheme 2. It is believed that the electrophilic attack of **11**/**12** on the ether oxygen, being a low activation energy pathway, should dominate the overall reaction pathway (vide infra). There are some supports on this proposal from the studies of 2,5-cyclohexadienon-4-ylidenes; these ketocarbenes, while exhibiting mostly triplet ground-state physical phenomena at a low temperature,[4,16] show a tendency to react as their singlet with olefins,[1] arenes,[18] and nonbonded electron pairs[5] under ordinary preparative reaction conditions. While the recent studies by flash photolysis at ambient temperatures[5] indicate that the reactions of these ketocarbenes exhibit a more complex pattern than those proposed,[1] the result described here shows well-manifested electrophilic reaction of the allied carbenoids.

Both singlet states **10** and **11**/**12**, in Scheme 2, are electrophilic at C-2 to attract the attack of the lone pair electrons of the THF oxygen. While the attack on **11**/**12** must occur at the σ-orbital, that on **10** at the p-orbital, since both types of orbitals are unoccupied orbitals. The latter attack involving **10** is unlikely, not only for the energetic reason discussed above but also since it must proceed by a series of complex events including an orbital inversion to allow azulenolate delocalization. The stabilized oxonium azulenolate **13** from the singlet state **11**/**12** is the key intermediate that is followed by one or more nucleophilic THF attacks at the α-position of the oxonium center as the chain propagation step to give **14**. It follows that the orientation of azulenolate anion and the oxonium center in **14** determine the probability of a ring closure to form the macrocyclic polyether bridge; that is, the conformation and stability of **14** are the factors to control the polyether ring size. The preferred size of polyether bridges at 13–16 members for **5** indicates that the conformations of **14** at $n = 1$ and 2 are the best stage where the azulenolate can attack the oxonium α-position in competition against an intermolecular propagation step of the THF attack. The preference to span an 11-membered bridge over a 16-member one in **5c-2THF** is puzzling and will be commented later. The propensity of electrophilic attacks of 2,5-cyclohexadienone-4-ylidenes has been reported and has demonstrated the highly electron-deficient nature of these carbene centers;[18] in effect, this deficiency is reinforced by the conjugation with an electron-withdrawing carbonyl group. This reactivity is in sharp contrast to α-ketocarbenes and cycloheptatrienylidene[15] that are shown to be weakly nucleophilic species.

Having established a singlet state mechanism for spanning an ether bridge, the poor yields of **5c-2THF** in the photolysis of diazo azulenoquinone **3c** could be ascribed to steric hindrance by the two vicinal carboxylate groups. But the preferential formation of the 11-membered ether bridge is unsettling, particularly when compared to the photolysis products of **3a** and **3b** in which the corresponding products with 2THF incorporation constitute minor quantities in comparison to those

---

[17] (a) Durr, H. *Fortschr. Chem. Forsch.* **1973**, *40*, 103. (b) Sole, A.; Olivella, S.; Bofill, J. M.; Anglada, J. M. *J. Phys. Chem.* **1995**, *99*, 5934.

[18] (a) Dewer, M. J. S.; Narayanaswami, K. *J. Am. Chem. Soc.* **1964**, *86*, 2422. (b) Baldwin, J. E.; Smith, R. A. *J. Am. Chem. Soc.* **1967**, *89*, 1886.

with 3THF, i.e., **5a-3THF** and **5b-3THF** are the major products. Most 1- and 3-carboxylate groups in azulene derivatives published previously[6,7] and here showed low $\nu_{C=O}$ stretching frequencies in the vicinity of the 1660−1690 cm^{-1}, indicating extensive conjugation with the electron-rich five-membered ring; this necessitates a coplanar orientation of the ester and five-membered ring. Such a coplanar conformation is also indicated by the unusually low NMR doublet chemical shifts of H-8 in 1-carboxylate-substituted azulenes as shown above and in the literature.[6,7] This conformation, when applied to the mandatory intermediate of conjugated ketocarbene with 1,3-dicarboxylate substitutions in the valence isomers in Scheme 2, could predict two types of steric hindrance in the ether bridge spanning process. First, the approach of THF oxygen lone-pair electrons to the empty σ-orbital of the **11c**/**12c** pair is severely hindered; in comparison, that to the p-orbital in **10c** can hardly encounter any hindrance. Secondly, the oxonium side chain in **14** must circumvent the 3-carboxylate group to receive the electrophilic attack of the azulenolate center at the α-carbon to the oxonium center, i.e., to complete the ring closure of intermediate **14**; such a hindrance obviously does not operate here as indicated by the small 11-membered ring closure (see below). An extensive operation of the former type of hindrance at the C-2 σ-orbital is clearly indicated by the only 17% yield of **5c-2THF**, which also suggests that the singlet reacting species is **11**/**12**, but not **10**, since the approach to the p-orbital is not as hindered.

As the singlet pathway is retarded, the triplet reaction of the **8c**/**9c** resonance hybrid by hydrogen abstraction (i.e., to give **6** and **7**) should become more important and dominate the overall pathway (vide supra). The abstraction of an α-hydrogen of THF by the triplet state **8c**/**9c** can occur by the delocalized radical center at the p-orbital (i.e., azulenoxy radical), the approach of which is relatively free from steric hindrance imposed by the 1,3-dicarboxylate groups; subsequently, the radical pair **15** collapses preferentially by disproportionation to give **7** as the major product rather than by the radical combination to give **6** since the approach of radical centers in **15** should encounter hindrance from the 1,3-dicarboxylate groups. The allied radical addition and reduction products from solvents have been found as minor products in a number of previous photoreactions of azulenoquinone diazides.[6a,7c] Returning to the formation of **5c-2THF**, some kinds of steric effects must exist to discourage an intermolecular THF attack on oxonium ion **14** at the two THF stage ($n = 1$) and/or to facilitate the azulenolate intramolecular attack on the α-carbon to the oxonium center; undoubtedly, such effects must be caused by the C-4 carboxylate group and regulate the polyether size to give **5c-2THF**.

The intuitive electronic isomerism proposed in Scheme 2, while satisfactorily explaining the observed chemical reactions, must be compared and reconciled with the detailed ab initio MO studies[17b] of 2,5-cyclohexadienone-4-ylidene published recently by Olivella's group. The studies show that while, as expected, the electronic ground state is the lowest triplet species, the conventional closed-shell singlet carbene is calculated to have a substantially high energy level by 22 kcal/mol above the ground state. The latter singlet corresponds to our singlet **10**, which has been regarded to be a high energy species and eliminated as a possible reacting species. The lowest singlet state is predicated to be an open-shell singlet species that lies much closer to the ground triplet state. Noting the conclusions of the highly delocalized electron and phenolate-like structure of this singlet, we may liberally interpret these to represent a singlet with highly delocalized electron cloud that coincides with the singlet p^2-state except that the single electron model is used in Olivella's calculation; this species corresponds to **11**/**12** in Scheme 2. Within this approximation, the proposal outlined in Scheme 2 is in good agreement with the theoretical study.[17b]

The reaction of 2,4-keto carbenes with cyclic ethers shown in Scheme 2 is a general method to span a polyether bridge across the reaction termini, in which 1,3-cyano and carboxylate groups should perturb the reaction pathway significantly by exerting steric as well as electronic effects as discussed above. An inspection of the literature reveals that the photolysis and thermolysis of substituted 1,4-benzoquinone diazides in THF[19] have been shown to give approximately 1:1 copolymers derived from the corresponding ketocarbenes and THF with molecular weights ranging, in some cases, from 1400 to 700. A claim of a more complex reaction pattern in a similar investigation[20] lacks details to rationalize the reported product structures. There is ample room to explore the potential of this type of reactions, in particular, in the area of the effects of substituent effects on the pathway of macrocycle ether formations.

The macrocyclic polyethers **5** possess an elliptic cavity, part of which is surrounded by an azulene nucleus; the estimated cavity diameters estimated from the available X-ray structures give a range of 6.4−4.1 Å (long-short distances) for **5a-2THF** and 7.3−6.6 Å for **5a-2THP**, others posses intermediate figures. Most polyethers **5**, except **5a-3THF**, exhibit one face of the macrocycle relatively open with respect to the other face, owing to an inclined conformation of the azulene ring with a smaller cyano group preferentially pointing to the inside of the cycle (Figure 1). Indeed, **5a-2DXN** has been shown to be able to complex with various alkaline metal ions, K$^+$, Na$^+$, and Li$^+$ ions, and also to exhibit fluorescence from the azulene moiety.[21] Such compounds are potentially useful molecular devices for responding and registering the environmental changes using light absorption and/or emission as the source of information indicators. However, the coordinating sites in these polyethers **5** with THF and THP units are few and far between alkyl chains; these compounds provide a new type of macrocyclic ligands.

Conjugated ketocarbenes are generally described to react by insertion and radical mechanisms and to have a triplet state in the lowest ground state.[1−5] In contrast, the present work shows that the allied ketocarbenes can react readily from their singlet state and by a stepwise electrophilic mechanism with an ether C−O bond; this provides another general reaction pattern.

---

(19) (a) Kunitake, T.; Price, C. C. *J. Am. Chem. Soc.* **1963**, *85*, 761. (b) Stille, J. K.; Cassidy, P.; Plummer, L. *J. Am. Chem. Soc.* **1963**, *85*, 1318.

(20) Plekhanova, L. G.; Nikiforov, G. A.; de Jonge, C. R. H. I.; Ershov, V. V. *Izv. Akad. Nauk. SSSR, Ser. Khim.* **1980**, 136 and the related papers cited herein.

(21) Chang, T. C.; Lin, Y. S.; Chow, Y. L. Unpublished results from this laboratory.

Experimental Section

Unless stated otherwise, materials and instruments were the same as those described in the previous paper.[6] Photolysis was carried out in a Rayonet Irradiator (RPR-100) equipped with 16 RPR 3000 Å lamps and a bottom fan. NMR spectra were taken in $CDCl_3$ except **3a** and **3c**, UV−visible spectra in chloroform and IR spectra in KBr disks.

Preparation of Azulenoquinone Diazides. To a dioxane (6 mL) solution containing **4a** (1 mmol, 256 mg) and concd sulfuric acid (1 mL) stirred and cooled in an ice bath was added an aqueous solution (2 mL) of $NaNO_2$ (1.2 mmol, 83 mg) slowly dropwise to maintain a temperature of approximately 0 °C over 20 min. After being stirred at 0 °C for 2 h, the solution was diluted with a large amount of ice (50−100 mL) and allowed to warm to room temperature. The precipitated orange crystals **3a** were filtered. Additional crystals were obtained by extraction of the aqueous layer with $CHCl_3$ and the workup of the extracts; **3a** (a total yield of 250 mg, 99%) was soluble in most solvents and kept under dark cover before use without further purification: mp 169−170 °C dec; ^{1}H NMR (DMSO-d_6) δ 4.00 (s, 3H), 6.63 (t, J = 10.6 Hz, 1H), 6.74 (d, J = 12.3 Hz, 1H) 6.99 (t, J = 8.5 Hz, 1H), 8.18 (d, J = 11.8 Hz, 1H); ^{13}C NMR (DMSO-d_6) δ 52.6, 67.2, 103.5, 113.4, 118.2, 126.3, 130.4, 130.6, 133.7, 136.4, 136.9, 161.2, 181.3; UV−vis ($CHCl_3$) λ_{max} (log ϵ) 455 (3.74), 395 (3.63), 312 (3.73) nm; IR (KBr) 2180, 2170, 1708, 1673, 1579, 1307, 1108 cm^{-1}; MS (EI) m/e 253 (M^+, 60), 227 (50), 210 (22), 196 (92), 182 (40), 167 (100), 139 (80). Orange-red crystals **3c** were obtained by a similar process in 95% yield: mp 113−114 °C dec; ^{1}H NMR ($CDCl_3$) δ 3.95 (s, 6H), 6.55 (t, J = 8.0 Hz, 1H), 6.66 (d, J = 12.4 Hz, 1H), 6.88 (t, J = 12.4 Hz, 1H), 8.70 (d, J = 11.5 Hz, 1H); UV−vis ($CHCl_3$) λ_{max} (log ϵ) 427 (2.50), 375 (3.35), 326 (4.11) nm; IR (KBr) 2190, 1683, 1583, 1494, 1439, 1304, 1203 cm^{-1}; MS (EI) m/z 286 (M^+, 20), 260 (32), 228 (51), 197 (90).

Diazotization of solid **4b** (300 mg) wsa done differently: by suspension in CF_3CO_2H and addition of $NaNO_2$ solution (462 mg in 2 mL) at 0 °C. The solution was diluted with ice and worked up as above to give red-orange crystals **3b** (272 mg, 92%) that were isolated in a darkened area since they turned black on the surface by room light: mp 151−152 °C dec; ^{1}H NMR (DMSO-d_6) δ 6.69 (dd, J = 9.5, 9.7 Hz, 1H), 6.76 (d, J = 12.7 Hz, 1H), 7.02 (dd, J = 12.6, 8.5 Hz, 1H), 7.30 (d, J = 11.4 Hz, 1H); ^{13}C NMR (DMSO-d_6) δ 72.3, 98.8, 103.1, 112.0, 112.8, 126.9, 129.3, 133.7, 134.2, 134.8, 136.8, 180.7; UV−vis ($CHCl_3$) λ_{max} (log ϵ) 452 (3.59), 391 (3.50), 312 (3.60) nm; IR (KBr) 2210, 2175, 1619, 1506, 1487, 1230, 1115 cm^{-1}; MS (EI) m/z 220 (M^+, 27), 194 (30), 164 (70), 137 (21).

Photolysis of Diazides 3a and 3b in THF. A dilute solution of **3a** or **3b** (100 mg) in dried THF (100 mL) contained in two Pyrex tubes (50 mL) was purged with dried nitrogen for 10 min and irradiated with RPR 3000 A lamps for 6 h at about 30 °C. The reaction could be followed by TLC to see the decrease of **3**. The photolysates was evaporated, and the crude product was chromatographed to afford **5a-2THF** and **5a-3THF** as the products.

5a-2THF: 16% yield; mp 116−117 °C; ^{1}H NMR δ 1.72−1.84 (m, 4H), 1.99−2.07 (m, 4H), 3.34−3.41 (m, 2H), 3.57−3.66 (m, 2H), 3.94 (s, 3H), 4.34−4.37 (m, 1H), 4.51−4.55 (m, 1H), 4.71−4.76 (m, 1H), 5.32−5.37 (m, 1H), 7.37 (d, J = 11.0 Hz, 1H), 7.50 (t, J = 10.0 Hz, 1H), 7.72 (t, J = 10.8 Hz, 1H), 9.43 (d, J = 10.8 Hz, 1H); ^{13}C NMR δ 24.5, 25.4, 26.0, 27.3, 51.3, 69.2, 69.6, 72.7, 75.0, 85.9, 107.1, 117.9, 121.5, 128.1, 134.6, 136.2, 137.0, 139.7, 164.0, 164.6, 169.0; UV−vis ($CHCl_3$) λ_{max} (log ϵ) 465 (3.11), 364 (3.91), 336 (4.65) nm; IR (KBr) 2195, 1681, 1481, 1437, 1384, 1255, 1164 cm^{-1}; MS (EI) m/z 369 (M^+, 32), 297 (18), 225 (25), 211 (100), 149 (27), 127 (53); MS (FAB) 370.1 (M^+ + H); HRMS calcd for $C_{21}H_{23}O_5N$ 369.1576, found 369.1577.

5a-3THF: 71% yield; mp 111−112 °C; ^{1}H NMR ($CDCl_3$) δ 1.56−1.64 (m, 4H), 1.77−1.82 (m, 4H), 1.88−2.08 (m, 4H), 3.41 (t, J = 6.5 Hz, 2H), 3.48 (q, J = 6.3 Hz, 4H), 3.57 (t, J = 7.3 Hz, 2H), 3.94 (s, 3H), 4.45 (t, J = 5.3 Hz, 2H), 4.78 (t, J = 7.0 Hz, 2H), 7.29 (d, J = 10.8 Hz, 1H), 7.43 (t, J = 10.3 Hz, 1H), 7.70 (t, J = 10.8 Hz, 1H), 9.43 (d, J = 10.5 Hz, 1H); ^{13}C NMR ($CDCl_3$) δ 24.9, 25.3, 26.3, 26.5, 27.2, 27.7, 51.2, 69.7, 70.2, 70.4, 70.7, 70.9, 74.5, 84.9, 105.4, 115.8, 117.6, 126.7, 131.9, 136.3, 137.4, 139.3, 162.5, 164.7, 168.5; UV−vis ($CHCl_3$) λ_{max} (log ϵ) 465 (3.12), 358 (3.89), 318 (4.54) nm; IR (KBr) 2925, 2200, 1671, 1449, 1383, 1263, 1224, 1150 cm^{-1}; MS (EI) m/z 442 (M^+ + 1), 370 (25), 297 (100), 266 (60), 225 (33), 211 (94), 183 (63), 127 (40); MS (FAB) 442.1 (M^+ + H); HRMS calcd for $C_{25}H_{31}O_6N$ 441.2125, found 441.2148.

5b-2THF: 11% yield; mp 141−143 °C; ^{1}H NMR ($CDCl_3$) δ 0.89−1.83 (m, 10H), 3.33−3.39 (m, 2H), 3.53−3.61 (m, 2H), 4.73−4.79 (m, 2H), 7.41 (d, J = 11.3 Hz, 1H), 7.52 (t, J = 10.1 Hz, 1H), 7.78 (t, J = 9.9 Hz, 1H), 8.40 (d, J = 10.1 Hz, 1H); ^{13}C NMR ($CDCl_3$) 24.1, 25.1, 26.5, 29.6, 69.0, 69.3, 70.6, 72.4, 86.1, 86.5, 115.0, 116.6, 116.8, 122.5, 127.8, 135.1, 137.1, 140.6, 165.0, 169.1; UV−vis ($CHCl_3$) λ_{max} (log ϵ) 469 (2.74), 357 (3.62), 331 (3.83) nm; IR (KBr) 2915, 2200, 1609, 1443, 1409, 1263, 1197 cm^{-1}; MS (EI) m/z 336 (M^+, 27), 264 (17), 236 (40), 210 (100), 195 (29), 127 (38); MS (FAB) 337.1 (M^+ + H).

5b-3THF: 76% yield; mp 115−116 °C; ^{1}H NMR ($CDCl_3$) δ 1.46−1.60 (m, 4H), 1.79−2.05 (m, 8H), 3.37−3.42 (m, 4H), 3.51−3.56 (m, 4H), 4.48 (t, J = 5.1 Hz, 2H), 4.87 (t, J = 6.1 Hz, 2H), 7.31 (d, J = 11.2 Hz, 1H), 7.43 (t, J = 9.8 Hz, 1H), 7.74 (t, J = 10.7 Hz, 1H), 8.34 (d, J = 9.5 Hz, 1H); ^{13}C NMR ($CDCl_3$ 24.9, 26.1, 26.2, 26.5, 26.8, 27.1, 69.7, 70.2, 70.5, 70.6, 71.2, 73.4, 86.3, 86.7, 115.2, 116.2, 116.5, 126.5, 131.9, 135.3, 136.9, 140.7, 162.8, 168.5; UV−vis ($CHCl_3$) λ_{max} (log ϵ) 458 (3.10), 371 (3.41), 334 (3.36) nm; IR (KBr) 2915, 2200, 1479, 1451, 1415, 1340, 1271, 1213, 1119 cm^{-1}; MS (EI) m/z 408 (M^+, 12), 336 (27), 264 (100), 236 (22), 210 (49), 49 (6); MS (FAB) m/z 409.2 (M^+ + H); HRMS calcd for $C_{24}H_{28}O_4N_2$ 408.2049, found 408.2047.

Photolysis of Diazide 3c in THF. Diazide **3c** (100 mg) in THF (100 mL) was photolyzed and worked up in the same way to afford three products. **5c-2THF:** 17% yield; mp 152−153 °C; ^{1}H NMR ($CDCl_3$) δ 1.42−1.84 (m, 8H), 3.21−3.49 (m, 4H), 3.87 (s, 3H), 3.96 (s, 3H), 4.24 (m, 1H), 4.40 (m, 1H), 4.51 (m, 1H), 4.88 (m, 1H), 7.25 (d, J = 10.7 Hz, 1H), 7.42 (t, J = 9.9 Hz, 1H), 7.65 (t, J = 10.8 Hz, 1H), 9.42 (d, J = 10.7 Hz, 1H); ^{13}C NMR ($CDCl_3$) δ 25.9, 26.0, 26.6, 26.9, 51.2, 51.9, 69.8, 70.0, 74.7, 75.9, 106.1, 111.0, 119.6, 126.4, 130.7, 135.3, 136.5, 138.3, 163.2, 164.9, 166.2, 166.9; UV−vis ($CHCl_3$) λ_{max} (log ϵ) 480 (2.63), 372 (3.50), 319 (3.94) nm; IR (KBr) 2935, 1716, 1680, 1430, 1261, 1196 cm^{-1}; MS (EI) m/z 402 (M^+, 45), 371 (20), 330 (8), 298 (12), 244 (21), 212 (61), 184 (30), 127 (100); MS (FAB) m/z 403 (M^+ + H); HRMS calcd for $C_{22}O_7H_{26}$ 402.1679, found 402.1664.

The major product, **1,3-dicarbomethoxy-4-azulenol (7)**, was obtained in 36% yield: mp 201−202 °C; ^{1}H NMR ($CDCl_3$) δ 3.93 (s, 3H), 4.02 (s, 3H), 7.35 (d, J = 10.1 Hz, 1H), 7.38 (t, J = 11.6 Hz, 1H), 7.72 (t, J = 11.6 Hz, 1H), 8.58 (s, 1H), 9.62 (d, J = 10.6 Hz, 1H); ^{13}C NMR ($CDCl_3$) δ 51.2, 53.1, 112.4, 116.9, 126.1, 126.3, 130.1, 137.9, 139.6, 139.9, 142.3, 165.4, 169.7, 170.5; UV−vis ($CHCl_3$) λ_{max} (log ϵ) 427 (2.45), 375 (3.29), 326 (4.05) nm; IR (KBr) 2950, 1691, 1613, 1589, 1435, 1384, 1280, 1207 cm^{-1}; MS (EI) m/z 261 (M^+ + 1, 100), 228 (81), 197 (90), 169 (60), 113 (20); MS (FAB) m/z 261 (M^+ + H).

1,3-Dicarbomethoxy-2-(2′-furanyl)-4-azulenole (6) was obtained as a minor product in 19% yield: mp 185−186 °C; ^{1}H NMR ($CDCl_3$) δ 2.01−2.47 (m, 4H), 3.82−4.04 (m, 3H), 3.93 (s, 3H), 4.00 (s, 3H), 5.63 (t, J = 7.0 Hz, 1H), 7.11 (t, J = 9.2 Hz, 1H), 7.29 (d, J = 11.6 Hz, 1H), 7.56 (t, J = 11.6 Hz, 1H), 8.08 (d, J = 9.2 Hz, 1H); ^{13}C NMR ($CDCl_3$) δ 26.2, 29.7, 34.1, 52.0, 52.8, 69.2, 78.2, 108.7, 122.9, 124.6, 125.8, 135.3, 138.2, 138.3, 151.2, 169.0, 169.2, 171.1; UV−vis ($CHCl_3$) λ_{max} (log ϵ) 427 (2.39), 375 (3.24), 326 (3.99) nm; IR (KBr) 2945, 1718, 1617, 1453, 1393, 1294, 1198, 1095 cm^{-1}; MS (EI) m/z 331 (M^+ + 1, 18), 300 (17), 270 (22), 238 (50), 210 (40), 197 (24), 169 (15); MS (FAB) m/z 331 (M^+ + H); HRMS calcd for $C_{18}H_{18}O_6$ 330.1103, found 330.1103.

Photolysis of Diazide 3a and 3b in THP and DXN. Dilute solutions containing diazide **3** (100 mg) in respective solvents were purged with nitrogen and irradiated for 6 h. Chromatography of each crude product gave one major product in each case.

5a-2THP: 75% yield; mp 132−133 °C; ^{1}H NMR ($CDCl_3$) δ 1.58−1.94 (m, 13H), 3.39 (m, 4H), 3.96 (s, 3H), 4.55−4.68 (m, 3H), 7.27 (d, $J = 11.1$ Hz, 1H), 7.43 (t, $J = 9.8$ Hz, 1H), 7.70 (t, $J = 9.9$ Hz, 1H), 9.40 (d, $J = 9.9$ Hz, 1H); ^{13}C NMR (CDCl$_3$) δ 24.5, 25.2, 29.6, 30.5, 30.7, 31.7, 51.8, 71.4, 71.6, 72.7, 76.9, 87.4, 106.1, 118.9, 119.5, 128.3, 133.5, 138.6, 138.8, 140.5, 164.7, 165.4, 169.6; UV−vis (CHCl$_3$) $\lambda_{\max}$ (log ϵ) 468 (3.29), 363 (4.14), 318 (5.68) nm; IR (KBr) 2950, 2245, 1681, 1467, 1431, 1381, 1267, 1202, 1132 cm^{-1}; MS (EI) *m*/*z* 397 (M$^+$, 20), 280 (13), 243 (15), 225 (4), 211 (100), 183 (12), 149 (5), 127 (3); MS (FAB) *m*/*z* 398.1 (M$^+$ + H); HRMS calcd for $C_{23}H_{27}O_5N$ 397.1889, found 397.1891.

5b-2THP: 72% yield; mp 163−164 °C; ^{1}H NMR (CDCl$_3$) δ 1.36−1.90 (m, 13H), 3.33 (m, 4H), 4.60−4.86 (m, 3H), 7.32 (d, $J = 11.2$ Hz, 1H), 7.47 (t, $J = 9.8$ Hz, 1H), 7.75 (t, $J = 9.9$ Hz, 1H), 8.37 (d, $J = 11.2$ Hz, 1H); ^{13}C NMR (CDCl$_3$) δ 23.5, 25.2, 29.7, 29.8, 30.6, 30.7, 71.2, 71.6, 79.3, 79.7, 86.3, 86.7, 115.8, 117.0, 120.5, 128.8, 132.6, 136.4, 139.5, 141.6, 165.2, 169.4; UV−vis (CHCl$_3$) $\lambda_{\max}$ (log ϵ) 467 (3.40), 372 (4.20), 314 (4.81) nm; IR (KBr) 2929, 2217, 1596, 1454, 1274, 1203, 1112 cm^{-1}; MS (EI) *m*/*z* 364 (M$^+$, 27), 278 (22), 210 (100), 182 (19), 153 (8), 127 (14); MS (FAB) *m*/*z* 365 (M$^+$ + H).

5a-2DXN: 79% yield; mp 158−159 °C; ^{1}H NMR (CDCl$_3$) δ 3.44−3.70 (m, 12H), 3.95 (s, 3H), 4.35−4.45 (m, 2H), 4.52−4.68 (m, 2H), 7.24 (d, $J = 10.8$ Hz, 1H), 7.42 (t, $J = 10.1$ Hz, 1H), 7.71 (t, $J = 10.6$ Hz, 1H), 9.45 (d, $J = 10.3$ Hz, 1H); ^{13}C NMR (CDCl$_3$) δ 51.2, 68.2, 69.7, 69.9, 70.6, 70.8, 71.6, 71.7, 75.1, 89.9, 105.6, 115.9, 117.2, 126.5, 131.3, 136.7, 138.0, 138.9, 163.1, 164.3, 169.8; UV−vis (CHCl$_3$) $\lambda_{\max}$ (log ϵ) 483 (3.35), 361 (4.19), 314 (4.76) nm; IR (KBr) 2930, 2290, 1680, 1461, 1381, 1335, 1274, 1128 cm^{-1}; MS (EI) *m*/*z* 401 (M$^+$, 100), 370 (20), 314 (12), 225 (33), 211 (52), 117 (31); MS (FAB) *m*/*z* 402 (M$^+$ + H); HRMS calcd for $C_{21}H_{23}O_7N$ 401.1474, found 401.1472.

5b-2DXN: 76% yield; mp 201−202 °C; ^{1}H NMR (CDCl$_3$) δ 3.46−4.26 (m, 12H), 4.58−5.09 (m, 4H), 7.31 (d, $J = 11.1$ Hz, 1H), 7.44 (t, $J = 9.9$ Hz, 1H), 7.74 (t, $J = 9.9$ Hz, 1H), 8.35 (d, $J = 9.8$ Hz, 1H); ^{13}C NMR (CDCl$_3$) 68.7, 69.9, 70.2, 70.6, 71.3, 72.1, 72.2, 72.6, 86.5, 87.1, 115.0, 116.5, 118.7, 126.7, 131.6, 135.3, 136.9, 140.3, 164.0, 169.3; UV−vis (CHCl$_3$) $\lambda_{\max}$ (log ϵ) 471 (2.75), 370 (3.64), 317 (3.99) nm; IR (KBr) 2915, 2195, 1487, 1446, 1269, 1207, 1108 cm^{-1}; MS (EI) *m*/*z* 368 (M$^+$, 73), 325 (4), 298 (12), 280 (11), 254 (3), 236 (5), 210 (23), 180 (10), 152 (18), 117 (54), 84 (100); MS (FAB) *m*/*z* 369.1 (M$^+$ + H); HRMS calcd for $C_{20}H_{20}O_5N_2$ 368.1372, found 368.1374.

Acknowledgment. The authors wish to acknowledge generous financial support of this project provided by the National Science Council, Taipei, Taiwan. S.J.L. is grateful to National Youth Commission, Taipei, Taiwan, for the award of a postdoctoral fellowship 1996−97. Y.L.C. wishes to thank Yamkang University and the Foundation and Donors of Advancement of Outstanding Scholarship, Taipei, Taiwan.

Supporting Information Available: Tables 2−6 and Figure 2 describing the X-ray structural parameters (bond distances, angles and torsion angles) and ORTEP drawings of polyethers **5** and supporting ^{1}H NMR spectra of **3**−**7** (24 pages). This material is contained in libraries on microfiche, immediately follows this article in the microfilm version of the journal, and can be ordered from the ACS; see any current masthead page for ordering information.

JO971494U